Potentialities of glass air-clad micro- and nano-fibers for nonlinear optics

Aurélien Coillet, Guillaume Vienne, and Philippe Grelu

Micro- and nano-fibers constitute an attractive platform for testing nonlinear devices with millimeter size in a simple and flexible fashion, with potential applications in ultra-fast, all-optical communications. In this article, we present challenges that must be addressed and targets that can be reached using such a platform. We describe a tunable laser source capable of delivering pulses with kW peak power and sub-0.1 nm linewidth that is specially designed for the study of resonant devices such as the nonlinear loop resonator. Experimental and simulations results are presented for silica microfiber based nonlinear devices. The prospect of developing hybrid devices combining highly nonlinear glasses and silica fibers is supported by numerical simulations of the coupling between two nanofibers of largely different optical indices.

1 Introduction

For ultra-fast telecommunication systems, all-optical data processing functions such as signal regeneration, wavelength conversion, and dynamical switching are highly desirable [1–5]. To this avail, most research efforts are devoted to the development of complex technical platforms. These include planar waveguide technology with non-silica waveguides, from silicon [4, 5] to hybrid-organic waveguides [3], as well as photonic crystal fibers [6, 7]. Although these platforms appear to be very efficient and are amenable to industrial fabrication, the availability of simpler and more flexible platforms is particularly attractive at the lab scale. Micro- and nano-fibers (MNFs), whose properties include low loss, easy connection to fiber based systems and a large design flexibility make for such an elementary test platform enabling short-length nonlinear optical devices [8,9]. Let us note that microfiber structures could be made more rugged when embedded within an aerogel (index typically below 1.05), as recently demonstrated in Ref [10]. It remains to be seen whether propagation losses could remain low and alignments could be maintained after embedding.

In a single-mode air-clad MNF, the fraction of the evanescent field is relatively large, which allows very efficient light coupling between two MNF of the same material. Energy transfer close to unity can be achieved after a propagation distance of a few microns, and this is accomplished experimentally by simply putting two MNFs into contact. As a result

simple manipulations can be used to demonstrate micro-optical devices such as optical couplers and ring resonators [11]. At the same time, the strong optical mode confinement in an air-clad material of refractive index n provides an effective area of the order of λ^2/n^2 that drastically increases the effective non-linearity compared to other waveguides for the same material [12, 13]. This enables significant non-linear effects to occur on propagation lengths as short as a few millimeters. So far, nonlinear optical experiments with MNFs have addressed supercontinuum [14, 15] and third-harmonic generation [16]. Interferometric devices that require a fine control of the nonlinear phase shift, such as nonlinear interferometers [17, 18] and bistable optical devices [19, 20] are much more difficult to test and require specific laser sources of high stability. In addition, intense but slow thermally-induced nonlinearities are expected to come into play in miniature interferometric devices [4, 21, 22].

In Ref. [21], thermally-induced optical bistability was reported in a silica microfiber loop resonator and associated with a response time close to the millisecond. The experiment was performed in the quasi-cw regime, with sinusoidal modulation of the input and a power below 100 mW. It was clear that only thermal effects would play a significant role in the buildup of an effective nonlinearity. In order to become sensitive to the low intrinsic ultrafast Kerr nonlinearity of electronic origin in sillica, high-peak intensity short-pulse experiments should be conducted, as detailed in the present article. The pulsed laser source used to test the microfiber loop resonator should meet specific criteria in terms of pulse duration, peak power, spectral width and repetition rate. The design and realization of such a laser source, unavailable commercially, is described in Section 2. The experimental results reported using this laser source at the input of a silica microfiber non-linear ring resonator are reported in Section 3. The obstacles to the observation of optical bistability are analyzed, whereas observed side effects are reported. One of the most noticeable nonlinear side effect observed is third-harmonic generation.

Ideally, nonlinear MNF resonators should take advantage of highly nonlinear materials, such as tellurite and chalcogenide glasses, while retaining good connectivity to silica fibers. With this in mind, the last section is focused on the possibility of using highly non-linear glasses and studies numerically the specific coupling requirements between MNFs in hybrid devices.

2 Design of the pulsed laser

Studying non-linearity in resonant or interferometric optical devices requires adapted and finely tunable laser sources. The availability of all-fiber components and optical sources, together with the need to develop all-optical processing in the telecommuncation window, make 1.55 µm the central wavelength of choice. The optical device under study is a microfiber loop resonator similar to that described in Ref. [21]. The quality factor Q of such device lies typically in the range 10^3 to 10^4, whereas the free spectral range FSR is typically between 0.2 to 2 nm, and can be adjusted during the experiment. The moderate finesse of these devices, of the order of 10, allows for the optical decay time, whose order of magnitude is the product of the finesse by the round-trip time, to be kept below 100 ps. Such a decay time is compatible with high-speed all-optical processing, and makes microfiber loop resonators very different from microsphere and microdisk resonators that use whispering

gallery modes and are associated with decay times in the microsecond range [23, 24]. We note however that specific high-Q micro-coil resonators (i.e. broken micro-coil resonators) have been recently proposed theoretically as efficient nonlinear optical filters for NRZ (Non Return to Zero) optical data streams [25].

Naturally, the drawback of a short transit time, here around 100 ps, is that the corresponding traveled distance — around 20 mm in silica — is short to accumulate a significant nonlinear phase shift (in the order of one). This implies that either an intense pulsed-laser source, or a highly non-linear waveguide material be used. While it has been long-recognized that any viable all-optical data processing solution should rely on the availability of highly non-linear materials, to date synthesizing and integrating reliably such materials remains a challenge. For this reason, we have initially considered pulsed-laser testing experiments on silica microfiber resonators.

The maximum effective nonlinearity for an optimum diameter silica microfiber is $0.09\,\mathrm{W^{-1}m^{-1}}$ [12]. Accordingly, the accumulation of a significant nonlinear phase shift in a short — around a centimeter — length of silica microfiber requires the use of pulses with peak power in the order of 1 kW. At the same time, the pulsed source should be tunable across several resonances, and its spectral linewidth should be kept narrower than the width of one resonance of the microfiber cavity. We also have to consider thermal effects induced by the laser source. Contamination of air-clad microfibers during the fabrication process increases light diffusion and absorption significantly. Although losses can be generally considered small in terms of input to output power transfer, microfibers are vulnerable to heating induced by the input optical power in spite of their excellent contact surface-to-volume aspect ratio. A large input power, above 100 mW, is likely to break the microfiber which generally possesses a few hot spots. In pulse regime, high optical power transients can still be launched without damaging the microfiber, provided that the average power is kept typically below 50 mW [21]. The thermal response of the microfiber resonator will be an averaged one provided that the pulse duration is smaller than the typical thermal response (~ 1 ms) and that the source repetition rate is larger than the inverse of this thermal response time, namely above the kHz range. In addition, the pulse duration should be larger than the effective travel time in the resonator (finesse times round-trip time, typically) so that the pulse can significantly interfere with itself close to a resonance.

All these considerations lead to the following suitable features for the pulsed tunable laser source: pulse duration around 500 ps, repetition rate of 100 kHz, and peak power greater than 1 kW, for an averaged power around 50 mW. The spectral linewidth should be narrower than 0.1 nm. A laser source combining all these features is not available commercially. For instance, suitable duration and peak power can be achieved in Q-switched microchip lasers (QSML), but the associated linewidth is above 1 nm, and QSMLs are not tunable. Therefore, we use a strategy frequently adopted in optical communications, which is to start with a tunable continuous-wave laser-diode source of great spectral purity and stability, and to apply external electro-optical modulation to tailor Fourier-transform-limited pulses.

To build this source we start with a continuously-tunable, external-cavity laser diode (TUNICS-PRI, Photonetics) that features a spectral linewidth smaller than 0.02 nm and is widely tunable across $1490 - 1620$ nm. The whole set-up is schematically illustrated in Fig. 1. The laser diode source is followed by a pigtailed 10 GHz lithium-niobate electro-optic modulator driven by a 400-ps electric-pulse generator, which carves pulses in the

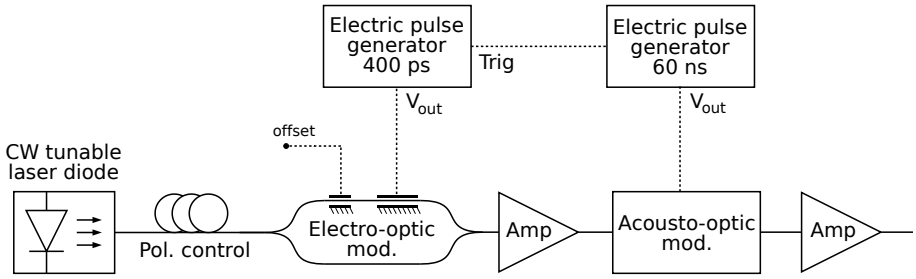

Figure 1: Sketch of the experimental pulsed laser source.

continuous beam at a 100 kHz repetition rate. The output signal is then sent to the first amplification stage based on a telecom erbium-doped fiber amplifier (23 dBm EDFA, Keopsys), giving an output peak power of 100 W. Due to the extinction ratio of the electro-optic modulator that is limited to 23 dB, the pulse signal is still polluted by a small continuous background which accounts for 98% of the total energy. Therefore, before sending the signal to the second amplification stage, most of the background is removed by an acousto-optic modulator synchronized with the electro-optic modulator, which opens a 60 ns gate in order to transmit the pulse and remove the remaining background elsewhere, with and extinction ratio greater than 40 dB. After that stage, more than 80% of the total energy is contained inside the 400 ps pulse. This situation represents a suitable input for the second amplification stage. The second optical amplifier uses highly-doped large-mode-area fiber technology to allow for 23 dB gain in a meter-long amplifying fiber, with minimal pulse distortion, and was manufactured by Keopsys Inc. As a result, the output pulse is a two-step pulse, resulting from the superposition of a low background on the 60 ns gate and the intense 400 ps pulse, which is 10^3 times more intense than the background, as displayed on Fig. 2 (a). The temporal pulse measurement is made with a 40 GHz sampling oscilloscope Tektronics CSA8200 equipped with a 30 GHz bandwidth optical input. Finally, the signal can reach 1.5 kW of peak power for a mean power of 80 mW while the spectral linewidth moderately broadens to 0.07 nm with the presence of a 50 cm long single mode fiber patchcord to connect the output of the second amplifier to an optical attenuator and then the input of the optical spectrum analyzer (see Fig. 2 (b)).

In addition to the narrow spectral line associated to the 400 ps pulse, the spectrum of Fig. 2 (b) features a broadband component that is attributed to the filtered amplified spontaneous emission of the second amplifier. However, this component is negligible since it lies 35 dB below the peak level.

This 400 ps pulsed source, featuring high spectral and temporal quality combined with its fine tunability in wavelength and power should allow us to study new microfiber nonlinear devices. Our first study is based on a silica loop resonator.

3 Testing of the silica loop resonator

The nonlinear response of a silica loop resonator was studied theoretically in Ref. [20], assuming continuous wave (cw) approximation and instantaneous response of the Kerr nonlinearity. Subsequent experiments in the quasi-cw regime have highlighted the importance of the thermal response [21], hence the present attempt to enter a nonlinear regime

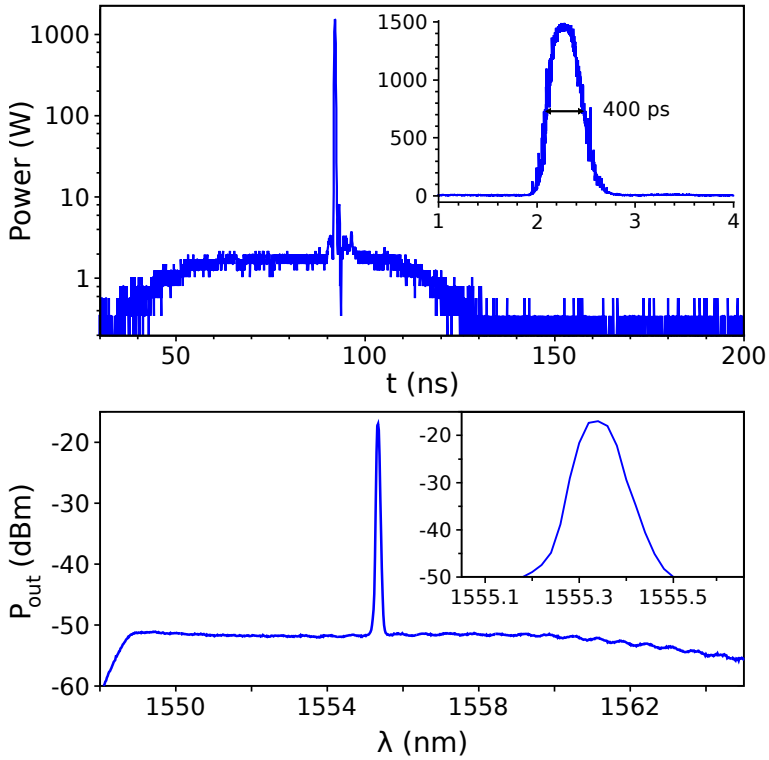

Figure 2: Measured pulsed-laser output: (a) temporal shape and (b) optical spectrum.

dominated by the instantaneous Kerr effect of electronic origin through the use of the 400 ps pulsed tunable source.

In practice, the ring resonator merely results from the twisting-and-folding of a silica microfiber into a loop held by van der Waals or electrostatic forces [26]. The contact between the adjacent sections of the fiber allows light to recirculate in the loop, creating a resonant cavity. When the intracavity intensity is high enough, the accumulated phase shift per roundtrip comprises a linear part and a nonlinear part:

$$\varphi = \beta L + \gamma_{eff} L |E_1|^2 \tag{1}$$

where β is the propagation constant, L the length of the loop, γ_{eff} the effective nonlinearity and E_1 the electric field inside the cavity.

Near resonance and for negative linear detuning, the nonlinear term can compensate part of the linear term, setting the light field closer to cavity resonance. This positive feedback mechanism leads to a subsequent increase of the intra-cavity intensity. As a result, cavity resonances are shifted from their linear locations and become asymmetric. This well-known mechanism can lead to optical bistability, when the cavity detuning is larger in magnitude than a critical value, and when light power exceeds a certain threshold [19, 20]. In a loop resonator at resonance, while the intracavity power is maximum, the transmitted optical power drops drastically. Using a pulse duration much larger than the cavity response time, as in the present studies, a strong pulse shaping effect is expected to occur close to resonance, since the transmission function of the resonator will respond almost instantaneously to the variation of the optical power along the pulse.

We have simulated such expected pulse shaping effects, considering various detunings between the pulse central frequency and one linear resonance of the loop resonator. Results are summarized in Fig. 3. The parameters used for this simulation are realistic compared to the features of microfiber loop resonators that can be achieved experimentally [26]. We assumed a 1.1 µm diameter silica microfiber, which is close to the single mode cutoff for a wavelength of 1.55 µm. The coupling factor between the two parts of the loop that are in contact is $K = 0.8$, the transmission loss factor through the coupling region is $a = 0.95$, and the effective nonlinearity is $0.09\,\mathrm{W}^{-1}\mathrm{m}^{-1}$. We can see in Fig. 3 the importance of the expected pulse shaping effects with respect to cavity detuning. Above a certain absolute value of the detuning, which is called the critical detuning, bistability occurs (Fig. 3 (e, f)) and creates asymmetry in the transmitted output. Below critical detuning, an important flat-topping that could be used in optical regeneration schemes (Fig. 3 (a, b)) occurs, as well as pulse splitting for larger detuning (Fig. 3 (c, d)). We see here that a key point is the control of the cavity detuning with respect to the laser input.

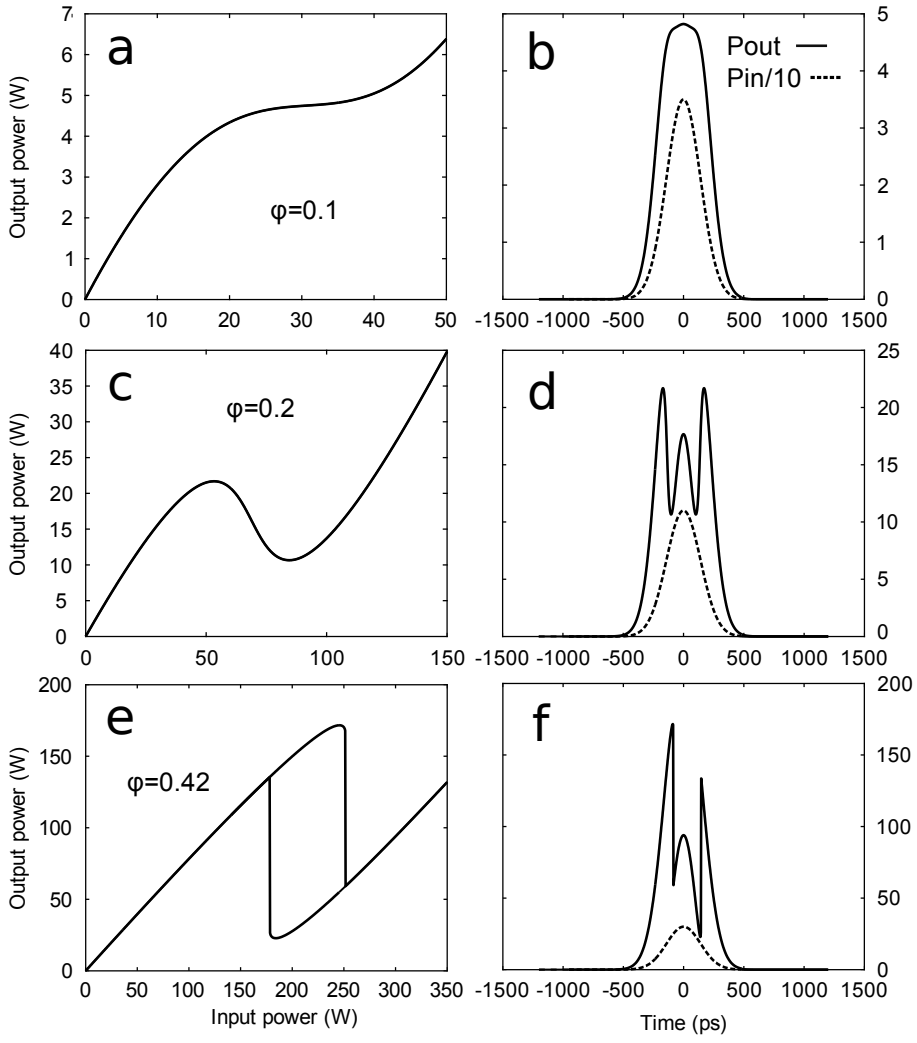

Figure 3: Simulated transfer function (a, c, e) and pulse shaping (b, d, f) through a nonlinear ring resonator for various linear detunings φ.

To make the silica microfiber loop resonator in practice, we used the flame-brushing technique [27] to fabricate low-loss biconic microfibers with diameters around 1 µm. The tapered part is slightly twisted so that it naturally folds into a loop whose diameter is close to 1 mm. This diameter can be subsequently modified by adjusting the pulling force onto the structure. One fiber end, before the tapering region, is connected to the 400 ps-laser source while the other end is connected to the analyzing device — spectrum analyzer or fast sampling oscilloscope. A typical transmission spectrum is shown on Fig. 4. The peak corresponds to the transmitted pulse, whereas the transmission of the broadband background of small amplitude that was observed on Fig. 2 (b) is now used to determine the linear characteristics of the loop resonator. The fitting of the latter spectral component yields $K = 0.44$ and $a = 0.85$, values that are below those used in Fig. 3. Anyway, using these new data in the simulation showed that 800 W of peak power would be enough to get significant pulse deformation at the output of the loop resonator.

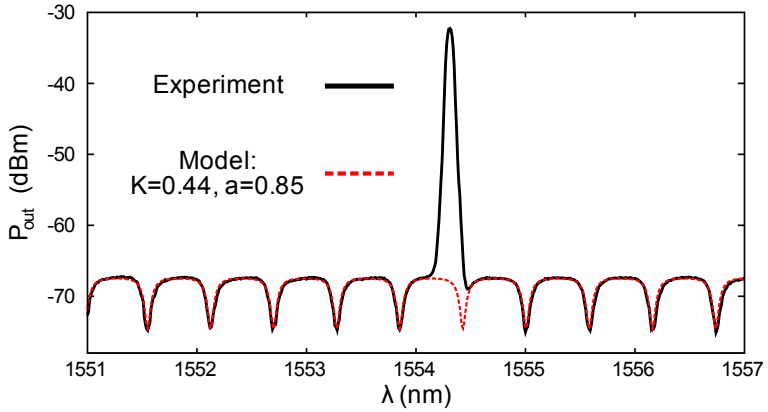

Figure 4: Experimental transmission spectrum and fit for a 2.7 mm diameter silica loop resonator. The ASE of the source is used to obtain this spectrum, and the large peak is due to the laser emission.

While increasing the input power, we did observe large pulse deformations, however they did not behave as expected when the laser wavelength was changed — that is equivalent to changing the cavity detuning. Instead of displaying a symmetric shape in the initial stages as in Fig. 3, the pulse splits and the relative peak powers of the two resulting parts change with the wavelength, as shown in Fig. 5 (a).

We have attributed the major part of this phenomenon to spectral broadening induced by self phase modulation (SPM) that can take place in three consecutive parts of the fiber setup, located before the loop resonator: the fiber output of the amplifier (30 cm), the connected buffer fiber (SMF) (1 m) and the 1 cm long tapered microfiber part that is located before the loop resonator.

An example of spectral broadening due to SPM, which produces effects close to those of Fig.5 (a) is shown in Fig. 5 (c). It was calculated using the experimental pulse shape with 1.5 kW peak power, and we needed to accumulate SPM through 4 m SMF, around twice the actual length of the propagation link. The spectral width becomes close to 0.1 nm, which is the typical full width at half maximum of the resonance dips. Therefore, the quasi-monochromatic assumption clearly breaks down. The wavelength near the leading edge is slightly higher, whereas it is lower on the trailing edge, and the transmission is

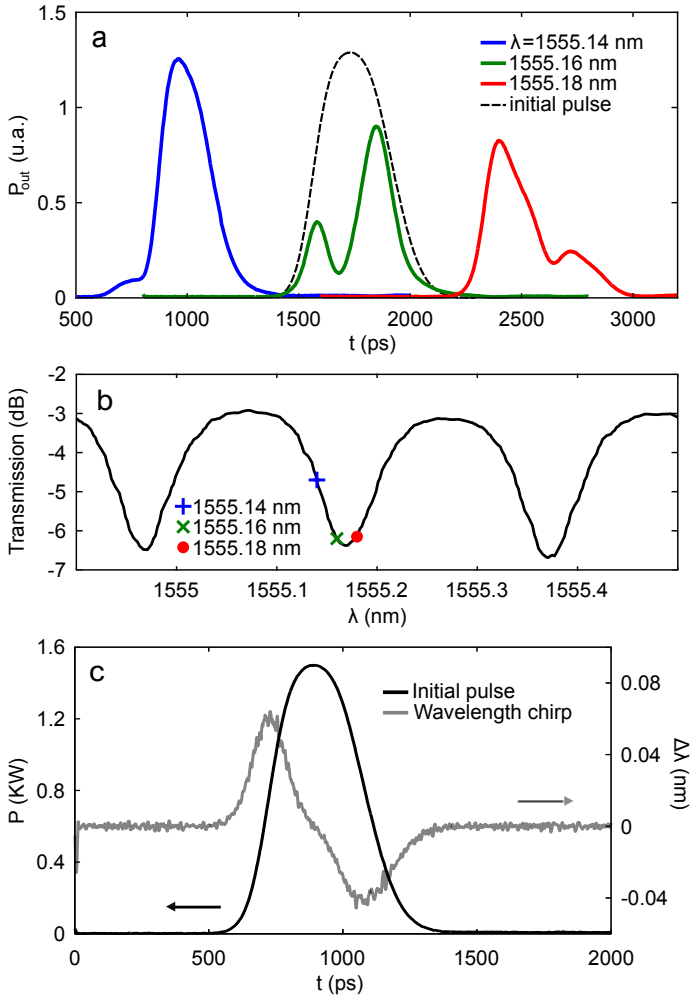

Figure 5: a) Experimental output pulse for 3 different pulse wavelengths, making 3 different cavity detunings. This asymmetric pulse shaping is explained with SPM broadening. b) Experimental transmission spectrum of the resonator with respective positions of the central wavelength. c) Calculated SPM wavelength chirp taking into account experimental pulse shape and input power.

changed accordingly. For instance, for a central wavelength at 1555.16 nm (green X mark on Fig. 5 (b)), the wavelength corresponding to the middle of the pulse is in a spectrum dip, whereas the leading and trailing edges correspond to wavelengths less attenuated. The pulse is therefore reshaped and split into two parts. Moreover, frequency chirping of the pulse leads to a non-symmetric deformation. Hence, we believe the reshaping of Fig. 5 (a) can be for an important part attributed to the nonlinear phase shift occurring in the connecting fibers and microfiber, in conjunction with the linear spectral filtering of the resonator. Although there should be sets of parameters for which the effect of the SPM accumulated prior to the resonator would be small, i.e. when the resonator is chosen with a large free spectral range or small quality factor, those parameters would also be detrimental to the observation of a nonlinear effect from the resonator itself. As was stated from the beginning, the viable alternative is to use a highly nonlinear resonator material

to decouple the transport of light pulses from their processing.

As an interesting side nonlinear effect occuring in the microfibers, we observed that the silica microfibers produced a relatively important amount of third-harmonic generation (THG) when the peak power was above 1 kW, either in straight taper or in resonator configuration (Fig. 6 (a)). Indeed, a greenish color diffusing from the microfiber was visible with the naked eye, and we obtained a green beam at the output of the taper that could be spectrally analyzed. Using the tunability of our pump source, we were able to produce a green beam with a wavelength tuned from 516 to 521 nm and an average power of around 15 nW.

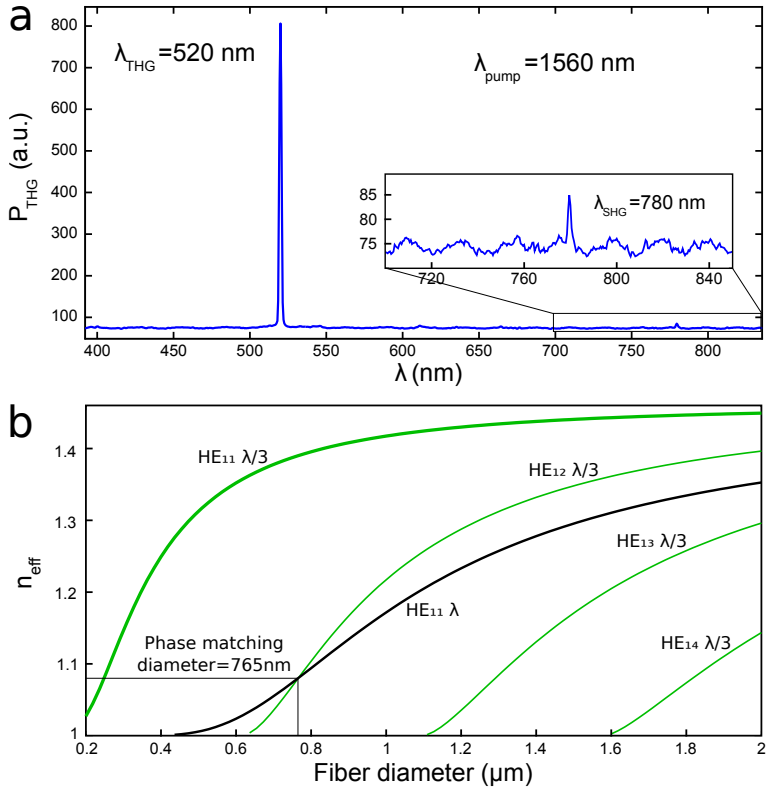

Figure 6: a) Output spectrum in the visible domain, showing strong third-harmonic generation. The microfiber used was around 700 nm in diameter at the waist, and 2 cm in length. b) Calculated effective indices for the different modes at play. For a pump wavelength λ =1550 nm, the phase-matching diameter is 765 nm.

To our knowledge, there has been only one previous report of such effect within silica microfibers [16]. Our results are in good correspondance with the experimental results reported by Grubsky *et al.* at the wavelength of 1064 nm. In addition to the wavelength difference, the most notable feature in our work is that microfibers were manually drawn, without any complex computer control, and the phenomenon still showed good reproducibility. In Ref. [16], THG was explained as resulting from phase-matched interaction between the HE_{11} fundamental wave and the third-harmonic wave propagating on the HE_{12} mode. For a pump wavelength λ =1550 nm, we have calculated the effective indices for the pump first mode and the first HE_{1n} modes for the third harmonic. These indices are plotted on Fig. 6 (b), and the optimal microfiber diameter for efficient phase-matched

Table 1: Glasses properties

Material	Chem.	n	n_2 (m^2W^{-1})
Silica	SiO_2	1.45	2.6×10^{-20} [20]
Tellurite	TeO_2	2	5×10^{-19} [20]
Chalcogenide	As_2S_3	2.4	5×10^{-18} [29]

wavelength conversion is found at 765 nm. Although in practice, it is unlikely to stop the manual stretching with such a precise diameter, there will be usually two locations on the taper where this condition is met, provided that the waist diameter is smaller than the phase-matching diameter value. We believe this explains why, without a specific drawing apparatus, THG can still be routinely obtained with the drawing of a thin, low-loss microfiber, for instance with minimal diameter in the 700 nm range and total length around 2 cm. The experimental spectrum presented in Fig. 6 (a) also shows (inset) a small amount of second harmonic generation, which is believed to be caused by surface interaction. This phenomenom can also be phase-matched, with the HE_{21} 780 nm mode, as predicted by Grubsky.

Unfortunately, any further increase in power leads to damaging the structure, either by unfolding the loop through radiation pressure, or melting the microfiber when dust is stuck on it. Here, silica microfibers, due to the low intrinsic non-linearity of silica and the short interaction length of microfibers, seem to reach their limit in terms of nonlinear effects for ultrafast optical processing. The most promising way to proceed is to change material and to study highly nonlinear glasses in order to increase the effect while remaining well below the damage threshold. But as a result of the previous study, the propagation part and the nonlinear processing part should be made of different materials, hence the important issue of connectivity between micro- or nanofibers of significantly different optical indices.

4 Soft glasses perspectives for hybrid nonlinear devices

Tellurite glasses are oxide glasses made from tellurium dioxide and can contain various oxide compounds like sodium oxide, zinc oxide, magnesium oxide, while chalcogenides are synthesized from chalcogenide elements (sulphur, selenium, tellurium) and non-oxide elements such as gallium, germanium or arsenic. These soft glasses present a low viscous transition temperature, about 200 °C, which makes them suitable for drawing microfiber from bulk [28]. Their interest in our case mainly resides in their high linear and nonlinear indices (see Table 1), which allow for a tighter confinement and several orders of magnitude higher effective nonlinearity compared to silica.

The results of the calculation of the effective index and the effective nonlinearity, for the first guided propagation mode, when the waveguide diameter is varied, are displayed on Fig. 7, for three different waveguide materials: silica, tellurite (TeO_2), and As_2S_3, a typical chalcogenide glass. We used again the wavelength of 1.55 µm. The maximal values for γ_{eff} are 0.09 $W^{-1}m^{-1}$ for silica, 5 $W^{-1}m^{-1}$ fo tellurite and 58 $W^{-1}m^{-1}$ for chalcogenide, this maximum being reached for microfiber sizes close to the cut-off diameter.

Connecting these soft glass microfibers to standard equipment, geared for silica fibers, is an issue but this could be solved in an elegant fashion by coupling light from and back

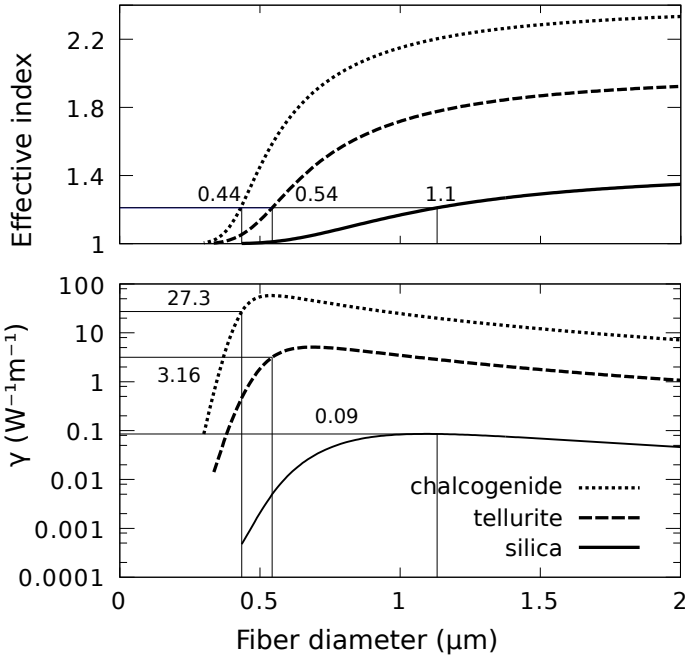

Figure 7: Calculated (a) effective index and (b) nonlinearity versus fiber diameter, for three different glasses, at a wavelength of 1.55 µm. The cutoff diameter of silica serves as a reference. Corresponding phase-matched diameters of chalcogenide and tellurite as well as corresponding effective nonlinearities are marked on the curves.

to silica microfibers via evanescent waves. Furthermore, this coupling would allow for the development of new hybrid structures such as a hybrid 4-port resonator [30] or a Mach-Zender interferometer, based on single-mode silica and soft glass microfibers. For this purpose, we need to find how to couple light from and to a silica 1.1 µm diameter with a chalcogenide ($n = 2.4$) or tellurite ($n = 2$) microfiber. This important issue has not been systematically addressed in previous literature.

The *a priori* condition would be to match the propagation constants of both microfibers, and to maximize the mode overlap, which should not be difficult considering that the microfibers with diameters below the single-mode cut-off have wide evanescent tails. Fig. 7 shows that the diameters for which the propagation constant matches the propagation constant of a 1.1 µm silica microfiber are 440 nm for chalcogenide and 540 nm for tellurite.

Such small diameters induce a lower confinement and effective nonlinearity, compared to the maximum occuring at the cut-off diameter, however it is still of the same order : 3.2 $\mathrm{W^{-1}m^{-1}}$ for tellurite and 27 $\mathrm{W^{-1}m^{-1}}$ for chalcogenide at phase-matching diameters. Such values for the effective non-linearity, combined with high coupling efficiency make it possible to realise hybrid nonlinear devices working at reasonably low peak power and very high bit rate.

Since the low index contrast approximation does not apply to our problem, an analytical calculation was out of reach and we performed numerical simulations by 3D FDTD, using the MIT's *Meep* software [31]. We have simulated the case of a chalcogenide microfiber coupling to a silica 1.1 µm diameter microfiber, the diameter of the chalcogenide microfiber

being increased from 340 to 500 nm. At the input (on the left in Fig. 8), light is launched from the chalcogenide microfiber. The coupling length was kept constant at 15 µm so that the periodic exchange between the two modes (if any) was visible. Fig. 8 (a) shows the index repartition in the symmetry plan and the intensity of the red color (online) on the images Fig. 8 (b) to (g) scales with the projection of the Poynting vector along the propagation axis.

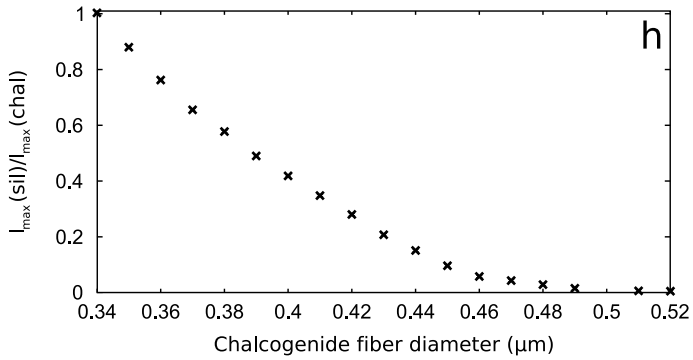

Figure 8: FDTD 3D simulations of the transmission between a chalcogenide fiber and a silica fiber. a) Index map (darker means higher index). b-g) Poynting vector along the propagation axis for increasing chalcogenide fiber diameter. The diameter of the output silica microfiber is 1.1 µm. h) Maximum intensity in the silica fiber divided by maximum intensity in the chalcogenide fiber versus chalcogenide fiber diameter.

Like in the low index contrast case, the simulations clearly show periodic energy exchange between the two waveguides along the coupling region. In principle, the coupling length has to be carefully tuned to get optimal efficiency [32]. As expected, the periodicity of energy exchange increases with an increasing phase mismatch between the two coupled modes, the phase-matched interaction corresponding to Fig. 8 (e). We notice however that the coupling efficiency increases with a decreasing diameter of the chalcogenide microfiber below the phase-matching diameter value, i.e. the effective index being lower in the input

fiber than in the output fiber. This behavior is in contrast with the expected behavior in the low-index contrast case, where propagation constants should match to get optimal energy exchange. Here, another phenomenon plays an important role: the overlap integral between the evanescent field produced by the chalcogenide nanofiber and the mode of the silica microfiber. The smaller the nanofiber, the larger the extent of the evanescent wave and the closer the propagation axes of both waveguides.

5 Summary

In this article, we have described a new laser source for studying nonlinear phase shift in interferometric or resonant microfiber devices. It emitted 400 ps pulses with more than 1 kW peak power, while the spectral linewidth was kept below 0.07 nm. This source was used to study the silica microfiber loop resonator, showing pulse shaping through the conjunction of SPM and of the narrow resonance transmission spectrum of the resonator. Silica microfibers also exhibited significant third-harmonic generation. The low intrinsic nonlinearity of silica however limits seriously obtainable phase shifts in short-length devices. Soft glasses such as tellurite and chalcogenide glasses would be very attractive, and integration with silica microfibers would allow the conception of original hybrid structures. We have shown numerically that, provided the diameters of the fibers are carefully chosen, efficient coupling could be achieved between waveguide materials of largely different indices. These new devices would pave the way for all-optical, fast operating functions for optical telecommunications such as demultiplexing, bistability, pulse shaping, and optical regeneration.

Acknowledgments

We were supported by the EGIDE program "Programme de Recherches Avancées Franco-Chinois" (project 15660SL), and by the Agence Nationale de la Recherche (project ANR05-BLAN-0152-01). G.V. gratefully acknowledges the support of the National Natural Science Foundation of China (Grant 60678039).

References

[1] O. Wada, "Femtosecond all-optical devices for ultrafast communication and signal processing," New Journal of Physics **6**, 183 (2004).

[2] J. K. Lucek and K. Smith, "All-optical signal regenerator," Opt. Lett. **18**, 1226–1228 (1993).

[3] C. Koos, P. Vorreau, T. Vallaitis, P. Dumon, W. Bogaerts, R. Baets, B. Esembeson, I. Biaggio, T. Michinobu, F. Diederich, W. Freude, and J. Leuthold, "All-optical high-speed signal processing with silicon-organic hybrid slot waveguides," Nature Photonics **3**, 216–219 (2009).

[4] V. R. Almeida, C. A. Barrios, R. R. Panepucci, and M. Lipson, "All-optical control of light on a silicon chip," Nature **431**, 1081–1084 (2004).

[5] R. Salem, M. A. Foster, A. C. Turner, D. F. Geraghty, M. Lipson, and A. L. Gaeta, "All-optical regeneration on a silicon chip," Opt. Express **15**, 7802–7809 (2007).

[6] P. S. Russell, "Photonic-crystal fibers," J. Lightwave Technol. **24**, 4729–4749 (2006).

[7] J. Travers, A. Rulkov, B. Cumberland, S. Popov, and J. Taylor, "Non-linear applications of microstructured optical fibres," Optical and Quantum Electronics **39**, 963–974 (2007).

[8] M. A. Foster, A. C. Turner, M. Lipson, and A. L. Gaeta, "Nonlinear optics in photonic nanowires," Opt. Express **16**, 1300–1320 (2008).

[9] G. Brambilla, F. Xu, P. Horak, Y. Jung, F. Koizumi, N. P. Sessions, E. Koukharenko, X. Feng, G. S. Murugan, J. S. Wilkinson, and R. D. J., "Optical fiber nanowires and microwires: fabrication and applications," Advances in Optics and Photonics **1**, 107–161 (2009).

[10] L. Xiao, M. D. Grogan, S. G. Leon-Saval, R. Williams, R. England, W. J. Wadsworth, and T. A. Birks, "Tapered fibers embedded in silica aerogel," Opt. Lett. **34**, 2724–2726 (2009).

[11] L. Tong and E. Mazur, "Glass nanofibers for micro- and nano-scale photonic devices," Journal of Non-Crystalline Solids **354**, 1240 – 1244 (2008). Proceedings of the 2005 International Conference on Glass - In conjunction with the Annual Meeting of the International Commission on Glass.

[12] M. A. Foster, K. D. Moll, and A. L. Gaeta, "Optimal waveguide dimensions for nonlinear interactions," Opt. Express **12**, 2880–2887 (2004).

[13] S. A. V. and T. M. Monro, "A full vectorial model for pulse propagation in emerging waveguides with subwavelength structures part i: Kerr nonlinearity," Opt. Express **17**, 2298–2318 (2009).

[14] R. R. Gattass, G. T. Svacha, L. Tong, and E. Mazur, "Supercontinuum generation in submicrometer diameter silica fibers," Opt. Express **14**, 9408–9414 (2006).

[15] D.-I. Yeom, E. C. Mägi, M. R. E. Lamont, M. A. F. Roelens, L. Fu, and B. J. Eggleton, "Low-threshold supercontinuum generation in highly nonlinear chalcogenide nanowires," Opt. Lett. **33**, 660–662 (2008).

[16] V. Grubsky and J. Feinberg, "Phase-matched third-harmonic uv generation using low-order modes in a glass micro-fiber," Optics Communications **274**, 447–450 (2007).

[17] N. J. Doran and D. Wood, "Nonlinear-optical loop mirror," Opt. Lett. **13**, 56–58 (1988).

[18] I. White, R. Penty, and R. Epworth, "Demonstration of the optical kerr effect in an all-fibre mach-zehnder interferometer at laser diode powers," Electronics Letters **24**, 340–341 (1988).

[19] H. M. Gibbs, *Optical bistability: Controlling Light with Light* (Academic Press, 1985).

[20] G. Vienne, P. Grelu, X. Pan, Y. Li, and L. Tong, "Theoretical study of microfiber resonator devices exploiting a phase shift," J. Opt. A: Pure Appl. Opt. **10**, 025303 (9pp) (2008).

[21] G. Vienne, Y. Li, L. Tong, and P. Grelu, "Observation of a nonlinear microfiber resonator," Opt. Lett. **33**, 1500–1502 (2008).

[22] X. Zeng, Y. Wu, C. Hou, J. Bai, and G. Yang, "A temperature sensor based on optical microfiber knot resonator," Optics Communications **282**, 3817–3819 (2009).

[23] M. L. Gorodetsky, A. A. Savchenkov, and V. S. Ilchenko, "Ultimate q of optical microsphere resonators," Opt. Lett. **21**, 453–455 (1996).

[24] D. K. Armani, T. J. Kippenberg, S. M. Spillane, and K. J. Vahala, "Ultra-high-q toroid microcavity on a chip," Nature **421**, 925–928 (2003).

[25] N. G. R. Broderick and T. T. Ng, "Theoretical study of noise reduction of nrz signals using nonlinear broken microcoil resonators," IEEE Photonics Technology Letters **21**, 444–446 (2009).

[26] M. Sumetsky, Y. Dulashko, J. M. Fini, A. Hale, and D. J. DiGiovanni, "The microfiber loop resonator: Theory, experiment, and application," J. Lightwave Technol. **24**, 242–250 (2006).

[27] L. Tong, R. R. Gattass, J. B. Ashcom, S. He, J. Lou, M. Shen, I. Maxwell, and E. Mazur, "Subwavelength-diameter silica wires for low-loss optical wave guiding," Nature **426**, 816–819 (2003).

[28] L. Tong, L. Hu, J. Zhang, J. Qiu, Q. Yang, J. Lou, Y. Shen, J. He, and Z. Ye, "Photonic nanowires directly drawn from bulk glasses," Opt. Express **14**, 82–87 (2006).

[29] G. Boudebs, F. Sanchez, J. Troles, and F. Smektala, "Nonlinear optical properties of chalcogenide glasses: comparison between mach-zehnder interferometry and z-scan techniques," Optics Communications **199**, 425–433 (2001).

[30] G. Vienne, A. Coillet, P. Grelu, M. E. Amraoui, J.-C. Jules, F. Smektala, and L. Tong, "Demonstration of a reef knot microfiber resonator," Opt. Express **17**, 6224–6229 (2009).

[31] A. Farjadpour, D. Roundy, A. Rodriguez, M. Ibanescu, P. Bermel, J. D. Joannopoulos, S. G. Johnson, and G. Burr, "Improving accuracy by subpixel smoothing in FDTD," Optics Letters **31**, 2972–2974 (2006).

[32] K. Huang, S. Yang, and L. Tong, "Modeling of evanescent coupling between two parallel optical nanowires," Appl. Opt. **46**, 1429–1434 (2007).